

CHAPTER 8

Vertical Variations of Fluid Velocities and Shear Stress in Surf Zones

Daniel T. Cox¹, Nobuhisa Kobayashi², and Akio Okayasu³

ABSTRACT: Detailed laboratory measurements are made of the velocity fluctuations to investigate the processes of the turbulence generation, advection, diffusion and dissipation in the surf zone. An order of magnitude analysis of the transport equation of the turbulent kinetic energy using the normalization adopted by Kobayashi and Wurjanto (1992) indicates an approximate local equilibrium of turbulence for shallow water waves in the surf zone. Estimates are found for common surf zone turbulence parameters. The calibrated values are used to show that the eddy viscosity varies gradually over depth and is nearly time-invariant and that the local equilibrium of turbulence is a reasonable approximation for spilling waves in the inner surf zone.

INTRODUCTION

The spatial and temporal variations of fluid velocities, shear stress, and turbulence intensity are required for a detailed analysis of sediment transport in the surf zone (Deigaard *et al.*, 1986). Field measurements of turbulent velocity fluctuations in the surf zone are difficult due to the harsh conditions for hot film anemometers and problems of calibration and voltage drift (George *et al.*, 1994). Laser-Doppler anemometry has been used in the laboratory (e.g., Stive, 1980; Nadaoka and Kondoh, 1982) to measure turbulent velocity fluctuations. However, no detailed analysis has been made of the turbulent kinetic energy transport equation in the nearshore region with laboratory data. Turbulence measurements in the surf zone are presented herein and are used to show that the local equilibrium of turbulence is a reasonable approximation for spilling waves in the inner surf zone. In addition,

¹Graduate Student, Center for Applied Coastal Research, University of Delaware, Newark, DE 19716 USA. Email: dtc@coastal.udel.edu Tel: +1 302 831 8477

²Professor and Associate Director, Center for Applied Coastal Research, University of Delaware, Newark, DE 19716 USA. Email: nk@coastal.udel.edu

³Assistant Professor, Department of Civil Engineering, Yokohama National University, 156 Tokiwadai, Yokohama 240, Japan. Email: okayasu@coast.cvg.ynu.ac.jp

the present analysis will be used to calibrate coefficients for the simple turbulence model for the surf zone.

TURBULENCE MODEL

The transport equation of the turbulent kinetic energy, k , is normally written as

$$\frac{\partial k}{\partial t} + u_j \frac{\partial k}{\partial x_j} = \nu_t \left(\frac{\partial u_i}{\partial x_j} + \frac{\partial u_j}{\partial x_i} \right) \frac{\partial u_i}{\partial x_j} + \frac{\partial}{\partial x_j} \left(\frac{\nu_t}{\sigma_k} \frac{\partial k}{\partial x_j} \right) - C_d^{3/4} \frac{(k)^{3/2}}{\ell} \quad (1)$$

where use is made of the repeated indices, $i = 1, 2$; t is time, $x_1 = x$ is the onshore directed horizontal coordinate; $x_2 = z$ is the vertical coordinate, positive upward with $z = 0$ at the still water level (SWL); $u_1 = u$ and $u_2 = w$ are the horizontal and vertical velocities; and σ_k is an empirical constant associated with the diffusion of k . The turbulent eddy viscosity, ν_t , may be expressed as (e.g., ASCE, 1988)

$$\nu_t = C_d^{1/4} \ell \sqrt{k} \quad (2)$$

in which ℓ is the turbulent mixing length, and C_d is an empirical coefficient.

The typical values of C_d and σ_k for *steady turbulent flow* are $C_d \simeq 0.08$ and $\sigma_k \simeq 1.0$ (Lauder and Spalding, 1972). The value of C_d is determined herein for normally incident waves on a rough, impermeable slope under the assumption of the approximate local equilibrium of turbulence. The equation for the dissipation rate of k might be used to estimate the turbulence length scale (k - ϵ model) but this equation is more empirical than (1) and gives only slightly better results for the case of bed shear stress calculations (Fredsoe and Deigaard, 1992). Alternatively, the mixing length ℓ in (2) may be specified simply as

$$\ell = \begin{cases} \kappa(z - z_b) & \text{for } z < (\overline{C_\ell} h / \kappa + z_b) \\ \overline{C_\ell} h & \text{for } z \geq (\overline{C_\ell} h / \kappa + z_b) \end{cases} \quad (3)$$

where κ is the von Karman constant ($\kappa \simeq 0.4$); z_b is the bottom elevation; h is the instantaneous water depth; and $\overline{C_\ell}$ is an empirical coefficient related to the eddy size. $\overline{C_\ell}$ is written with an overbar to show that it is time-invariant and to differentiate it from C_ℓ used later. Eq. (3) is similar to that used by Deigaard *et al.* (1986) for their analysis of suspended sediment in the surf zone in which use was made of $\overline{C_\ell} = 0.07$ and the mean water depth, \bar{h} , instead of the instantaneous depth, h . The use of h should be more appropriate in the swash zone in light of the limited field data of Flick and George (1990). Svendsen (1987) suggested $\overline{C_\ell} = 0.2$ – 0.3 for the steady undertow. The value of C_ℓ for the *unsteady* flow and the time-averaged value, $\overline{C_\ell}$, will also be determined for the present data.

The dimensionless variables are introduced following Kobayashi and Wurjanto (1992):

$$t' = \frac{t}{T}; \quad x' = \frac{x}{T\sqrt{gH}}; \quad z' = \frac{z}{H}; \quad u' = \frac{u}{\sqrt{gH}}; \quad w' = \frac{w}{H/T} \quad (4)$$

$$p' = \frac{p}{\rho g H}; \quad \nu_t' = \frac{\nu_t}{H^2/T}; \quad k' = \frac{k}{gH/\sigma}; \quad \ell' = \frac{\ell}{H/\sqrt{\sigma}}; \quad \sigma = \frac{T\sqrt{gH}}{H} \quad (5)$$

where the primes indicate dimensionless quantities, T and H are the characteristic wave period and height of the shallow water waves, and σ is the ratio between the horizontal and vertical length scales. The order of magnitude of k , ℓ , and ν_t is estimated such that the resulting normalized equations become consistent with the measured data as explained later.

Substitution of (4) and (5) into (1) under the assumption of $\sigma^2 \gg 1$ yields

$$\sigma^{-1} \left(\frac{\partial k'}{\partial t'} + u' \frac{\partial k'}{\partial x'} + w' \frac{\partial k'}{\partial z'} \right) = \tau' \frac{\partial u'}{\partial z'} + \sigma^{-1} \frac{\partial}{\partial z'} \left(\frac{\nu_t'}{\sigma_k} \frac{\partial k'}{\partial z'} \right) - C_d^{3/4} \frac{k'^{3/2}}{\ell'} \quad (6)$$

where the first and third terms on the right-hand-side are the production and dissipation terms, respectively. For their analysis of suspended sediment in the surf zone, Deigaard *et al.* (1986) used (6) in which the advection terms were neglected and the production of k' was estimated empirically. In short, they attempted to predict the variation of k' without analyzing u' , w' and τ' . Eq. 6 indicates that the production and dissipation of k' are dominant under the assumption of $\sigma^2 \gg 1$. This is qualitatively consistent with the findings of Svendsen (1987) who concluded that only a very small portion of the energy loss in the breaker (2-6% for the cases considered) was dissipated below trough level.

Considering the empirical nature of (6) with the coefficients σ_k and C_d as well as the uncertainty of the free surface boundary condition of k' even for steady turbulent flow (Rodi, 1980), (6) may be simplified further by neglecting the terms of the order σ^{-1} and the resulting equation is expressed in dimensional form as

$$\frac{\tau}{\rho} \frac{\partial u}{\partial z} \simeq C_d^{3/4} \frac{k^{3/2}}{\ell} \quad (7)$$

which implies the local equilibrium of turbulence. Substitution of $\tau/\rho = \nu_t \partial u / \partial z$ and (2) into (7) yields

$$k = |\tau| / (\rho \sqrt{C_d}) \quad (8)$$

$$\nu_t = \ell^2 \left| \frac{\partial u}{\partial z} \right| \quad (9)$$

With these assumptions, (8) is used to determine the appropriate value of C_d . Eq. (9) corresponds to the standard mixing length model (ASCE, 1988) and is used with (2) to determine C_ℓ and \overline{C}_ℓ in (3). The degree of the local equilibrium of turbulence is assessed using (7) with the calibrated coefficients C_d and \overline{C}_ℓ .

EXPERIMENT and DATA REDUCTION

The experiment was conducted in the 33 m long, 0.6 m wide and 1.5 m deep wave flume at the University of Delaware. A hydraulically actuated piston wavemaker

with a 1 m stroke was at the far end; and a rough, uniform 1:35 slope was emplaced at the near end of the flume. The water depth was 0.4 m in the constant depth section. Regular cnoidal waves were specified at the wavemaker, and the waves broke by spilling on the impermeable slope. The rough slope consisted of a layer of natural sand grains with median diameter $d_{50}=1$ mm glued to Plexiglas sheets and mounted on the entire slope. This was used to increase the bottom boundary layer thickness for estimating the bottom shear stress. A detailed analysis of the bottom shear stress outside and inside the surf zone is given in Cox, *et al.* (1995).

The free surface elevations were measured using capacitance-type wave gages with a sampling rate of 100 Hz. The velocities were measured using a two-component laser-Doppler anemometer with a pair of burst spectrum analyzers. The effective sampling rate was in excess of 1×10^3 data points per second, and the sampling rate was later reduced by band averaging to 100 Hz before the phase averaging procedure described below. The free surface and velocity fluctuations were measured at six vertical lines and are denoted L1, L2, . . . , L6 for brevity. The horizontal spacing of the measuring lines was on the order of 1 m, and the vertical spacing of the measuring points was on the order of 1 cm except near the bottom where measurements were made on the order of a fraction of the grain height, i.e. less than 1 mm. Details of the experiment are provided in Okayasu and Cox (1995).

The free surface and velocity measurements were reduced by a standard phase averaging procedure over 50 waves. The sampling interval was $\Delta t = 0.01$ s and the wave period was $T = 2.2$ s which gave $J = T/\Delta t = 220$ as the number of data points or phases per wave. The phase-averaged free surface elevations, η_a , were computed from the measured free surface, η_m , where the subscripts a and m refer to the phase-averaged and measured quantities. The variance of the free surface elevation, σ_η^2 , and the standard deviation, σ_η , were also computed. For the figures presented here, the phases are aligned with zero-upcrossing of the free surface elevation at $t = (T/4) = 0.55$ for the six measuring lines (Cox, 1995).

The normalization parameters for the turbulent quantities in (5) are given in Table 1 with the range of values for the measured data as explained later. The range is found by taking the minimum and maximum values for the phase-averaged quantities between the trough level and the bottom boundary layer which is defined simply as 1 cm above the impermeable bottom and consistent with the analysis of Cox (1995). The ranges given in parentheses are for the bottom boundary layer. The cross-shore locations of the measuring lines are given in Table 2 and are characterized as follows: L1 is seaward of the break point; L2 is at the break point which is defined as the start of aeration in the tip of the wave; L3 is in the transition region where the wave form goes from organized motion to a turbulent bore; and L4, L5, and L6 are in the inner surf zone where the saw-toothed wave shape is a well-developed turbulent bore (Cox, 1995). Table 1 indicates that the scaling of k , ℓ , and ν_i in (5) is appropriate inside the surf zone for L3 to L6.

Table 1: Range of k , ℓ , and ν_t for L1 to L6 and Normalization Quantities.

Line No.	k (cm ² /s ²)	gH/σ (cm ² /s ²)	ℓ (cm)	$H/\sqrt{\sigma}$ (cm)	ν_t (cm ² /s)	H^2/T (cm ² /s)
L1	0.2 – 2.8 (0.3 – 18.8)	684	0.60 – 1.20 (0.01 – 0.40)	3.04	0.11 – 0.61 (0.00 – 0.27)	79.4
L2	0.4 – 3.8 (0.4 – 35.9)	1007	0.60 – 1.91 (0.01 – 0.40)	4.19	0.17 – 1.03 (0.01 – 0.28)	132.9
L3	14.4 – 297 (4.9 – 45.6)	645	0.60 – 3.23 (0.01 – 0.40)	2.89	0.65 – 18.4 (0.01 – 0.76)	73.4
L4	20.7 – 559 (6.8 – 65.7)	337	0.61 – 4.26 (0.02 – 0.41)	1.68	0.81 – 34.8 (0.01 – 0.68)	30.9
L5	17.4 – 206 (4.1 – 35.6)	268	0.60 – 2.64 (0.01 – 0.40)	1.39	0.97 – 12.9 (0.01 – 0.60)	22.8
L6	13.9 – 179 (4.4 – 76.7)	162	0.61 – 2.00 (0.02 – 0.41)	0.91	0.81 – 11.1 (0.02 – 0.83)	11.6

Table 2 lists the free surface statistics for L1 to L6 where x is the onshore directed horizontal coordinate with $x = 0$ cm at L1; d is the distance below the still water level to the top of the Plexiglas sheet, i.e. the bottom of the 1 mm sand layer; H is the local wave height given by $H = [\eta_a]_{max} - [\eta_a]_{min}$ where the subscripts *min* and *max* indicate the minimum and maximum values of a phase-averaged quantity; $\bar{\eta}_a$ is the setup or setdown; $\bar{\sigma}_\eta$ is the time-average of the standard deviation of η_a ; and $[\sigma_\eta]_{min}$ and $[\sigma_\eta]_{max}$ are the minimum and maximum of the standard deviation values over the wave period. The cross-shore variations of $\bar{\eta}_a$, $[\eta_a]_{min}$, and $[\eta_a]_{max}$ have been well studied; however, less mention has been made of $\bar{\sigma}_\eta$, $[\sigma_\eta]_{min}$, and $[\sigma_\eta]_{max}$. From Table 2, $[\sigma_\eta]_{max}$ is very small for L1 indicating repeatability of the wave form. For L2, $[\sigma_\eta]_{max}$ increases slightly due to irregularities of wave breaking. For L3 in the transition region, $[\sigma_\eta]_{max}$ is at a maximum. For L4 to L6, $[\sigma_\eta]_{max}$ decreases with increasing distance to the shore. It is interesting to note the cross-shore variation of $[\sigma_\eta]_{max}$ because it could be used to better quantify the transition region of the surf zone (e.g., Nairn *et al.*, 1990 and references therein).

The signal dropouts are excluded in the phase averaging of the measured horizontal and vertical velocities. The phase-averaged horizontal and vertical velocities are denoted u_a and w_a , and the horizontal and vertical velocity variances are denoted σ_u^2 and σ_w^2 . The turbulent normal stresses may be assumed to be equal to $-\rho\sigma_u^2$ and $-\rho\sigma_w^2$ in the horizontal and vertical directions, where ρ is the fluid density. The phase-averaged covariance of the measured horizontal and vertical velocities is denoted σ_{uw} , and the turbulent shear stress, τ , may be assumed to

Table 2: Phase-Averaged Free Surface Statistics for L1 to L6.

Line No.	x (cm)	d (cm)	H (cm)	$\bar{\eta}_a$ (cm)	$[\eta_a]_{min}$ (cm)	$[\eta_a]_{max}$ (cm)	$\bar{\sigma}_\eta$ (cm)	$[\sigma_\eta]_{min}$ (cm)	$[\sigma_\eta]_{max}$ (cm)
L1	0	28.00	13.22	-0.30	-3.88	9.34	0.10	0.05	0.22
L2	240	21.14	17.10	-0.44	-3.60	13.50	0.14	0.06	0.98
L3	360	17.71	12.71	-0.05	-2.82	9.89	0.41	0.19	2.06
L4	480	14.29	8.24	0.20	-2.33	5.91	0.38	0.17	1.37
L5	600	10.86	7.08	0.75	-1.60	5.48	0.28	0.15	1.03
L6	720	7.43	5.05	1.13	-0.82	4.23	0.22	0.11	0.92

be equal to $-\rho\sigma_{uw}$.

Figure 1 compares the vertical variation of the Froude-scaled time-averaged horizontal turbulent intensity for the present measurements L3 to L6 with the data of George *et al.* (1994), Stive (1980), and Nadaoka and Kondoh (1982). The data of George *et al.* (1994) from their Figure 8a are for the natural surf zone and include random waves of both plunging and spilling type. The frozen turbulence assumption was used to extract the turbulent signal. The middle curve of George *et al.* (1994) indicates the mean value in several vertical bins and the envelope is this mean ± 1 standard deviation plus the uncertainty in the data reduction. The data of Nadaoka and Kondoh (1982) from their Figure 7 are for Case 1, spilling waves on a 1:20 slope, and include only the measuring lines inside the surf zone, i.e. P1 to P5. A frequency filter was used to extract the turbulent signal. It is noted that these data are plotted in Figure 1 using d rather than \bar{h} . The data of Stive (1980) are also taken from Figure 8a of George *et al.* (1994) and are presumably for Test 1, spilling waves on a 1:40 slope, and include the measuring lines in the transition region as well as the inner surf zone. Phase-averaging was used to extract the turbulent signal.

Only the data of George *et al.* (1994) are for multidirectional random waves measured in the field. The other three data sets are for normally incident, regular waves measured in the laboratory. The comparison of the present data set with that of Stive (1980) shows that the phase averaging method gives consistent results for laboratory waves of similar type. The comparison with Nadaoka and Kondoh (1982) indicates that the frequency filter may underestimate the turbulent signal as noted by other researchers (e.g., George *et al.*, 1994). Nevertheless, it would be useful to have a simple relation between the turbulent signals from the two methods since phase averaging cannot be used for random waves in a natural surf zone. Interpretation of the data of George *et al.* (1994) is difficult

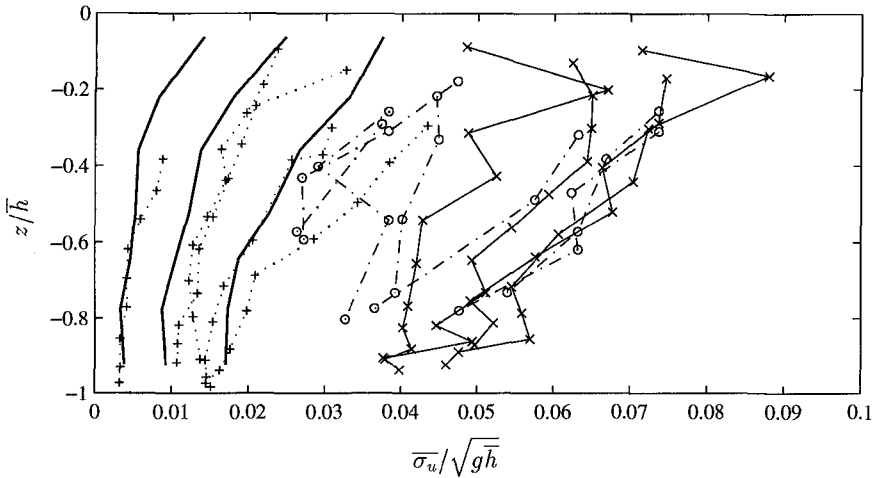


Figure 1: Comparison of Vertical Variation of Froude-Scaled Horizontal Turbulence Intensity with George *et al.* (1994) (—); Stive (1980) (\circ - - -); Nadaoka and Kondoh (1982) (+ ···); Present Data L3 to L6 (\times —).

because of the method used to extract the turbulent signal and because the waves were random and multidirectional. Clearly, more work is necessary in this area.

Figure 2 shows the temporal variations of the phase-averaged horizontal and vertical velocity variances, σ_u^2 and σ_w^2 , and velocity covariance, σ_{uw} , for five vertical elevations for L2. The five vertical locations for L2a to L2e are -5.04 , -13.04 , -17.04 , -20.04 , and -20.94 cm, respectively, where the still water level is $z = 0.0$ cm and the still water depth is $d = 21.14$ cm. Figure 2 shows almost no turbulence in the interior, and the turbulence seems to be confined to the bottom boundary layer. Also, as indicated in the caption, the proposed scaling may not be appropriate in the boundary layer outside the surf zone. The same quantities of Figure 2 for L2 are shown in Figure 3 for L4. The five vertical locations for L4a to L4e are -2.19 , -6.19 , -10.19 , -13.19 , and -14.09 cm, respectively, where the still water depth is $d = 14.29$ cm. This figure shows the spread and decay of turbulence generated by wave breaking. Also, the peak of the turbulence shifts downward. For L4a, the horizontal velocity variance is greater than the vertical variance over most of the wave period except at $t = 0.6$ s when the phase-averaged horizontal and vertical velocities are approximately the same (Cox, 1995). The proposed scaling indicated in the caption seems appropriate here. For L4c, the horizontal and vertical variances are approximately the same since the turbulence becomes more isotropic even though the vertical velocity is much smaller than the horizontal velocity at this elevation. For L4e, the horizontal variance is again

greater than the vertical variance since the vertical turbulent fluctuations may be limited by the solid boundary. Also, the covariance is negative for L4a to L4c.

Figure 4 shows the detail of the cross-shore variations of time-average horizontal and vertical variances, $\overline{\sigma_u^2}$ and $\overline{\sigma_w^2}$, and the time-averaged covariance, $\overline{\sigma_{uw}}$. Comparison of $\overline{\sigma_u^2}$ and $\overline{\sigma_w^2}$ for L3 to L6 shows that they are about the same magnitude below trough level and decay linearly downward except in the lower portion of the water column where $\overline{\sigma_u^2}$ remains approximately constant over depth and $\overline{\sigma_w^2}$ tends to zero near the bottom.

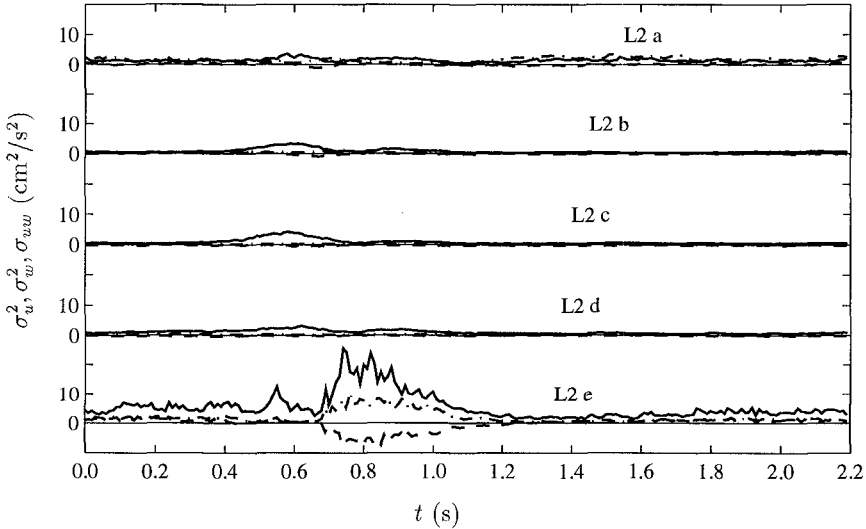


Figure 2: Temporal Variations of Phase-Averaged Horizontal Velocity Variance, σ_u^2 (—); Vertical Velocity Variance, σ_w^2 (---); and Covariance, σ_{uw} (- -) for Five Vertical Elevations for L2 with $gH/\sigma = 1007 \text{ cm}^2/\text{s}^2$.

ANALYSES OF WAVE GENERATED TURBULENCE

The dimensional shear stresses, τ_{ij} , are written in tensor notation as (e.g., Rodi, 1980)

$$\tau_{ij} = \rho \left[\nu_t \left(\frac{\partial u_i}{\partial x_j} + \frac{\partial u_j}{\partial x_i} \right) - \frac{2}{3} k \delta_{ij} \right] \quad (10)$$

where δ_{ij} is the Kronecker delta and k is the turbulent kinetic energy per unit mass which can be expressed in terms of the normal stresses as

$$k = -\frac{1}{2\rho} (\tau_{11} + \tau_{22} + \tau_{33}) \quad (11)$$

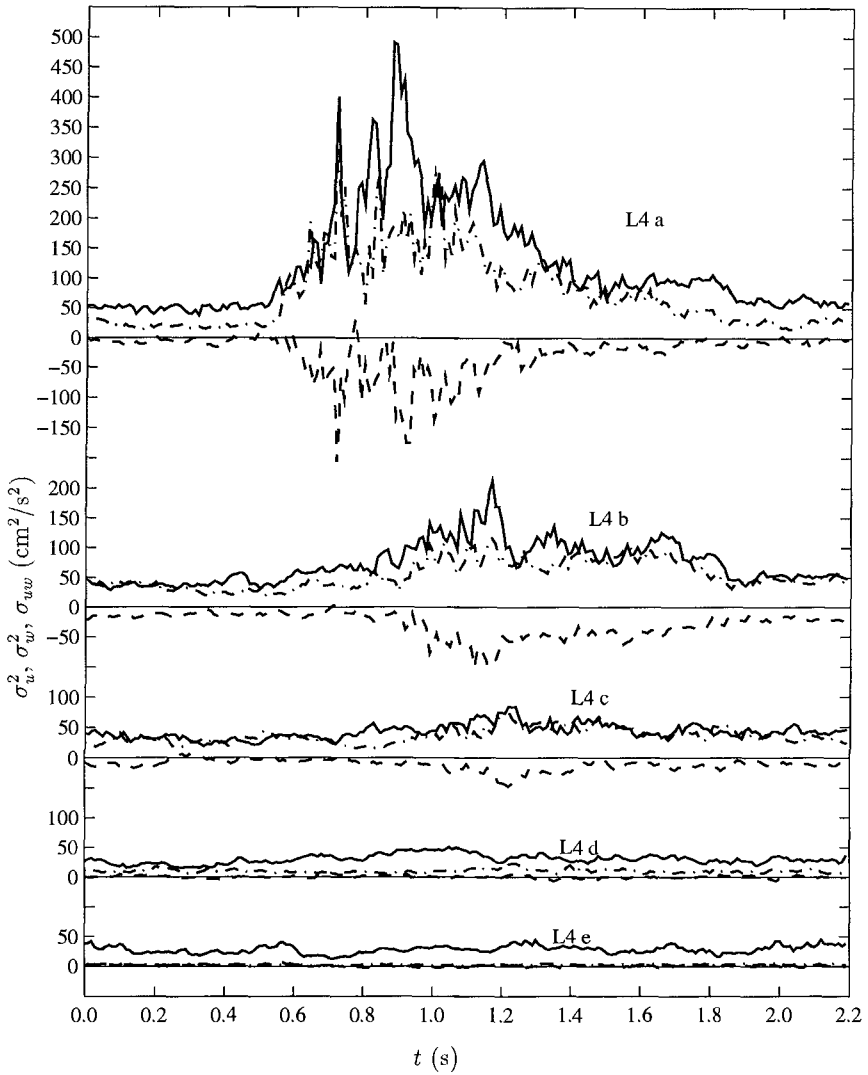


Figure 3: Temporal Variations of Phase-Averaged Horizontal Velocity Variance, σ_u^2 (—); Vertical Velocity Variance, σ_w^2 (- - -); and Covariance, σ_{uw} (- · -) for Five Vertical Elevations for L4 with $gH/\sigma = 337 \text{ cm}^2/\text{s}^2$.

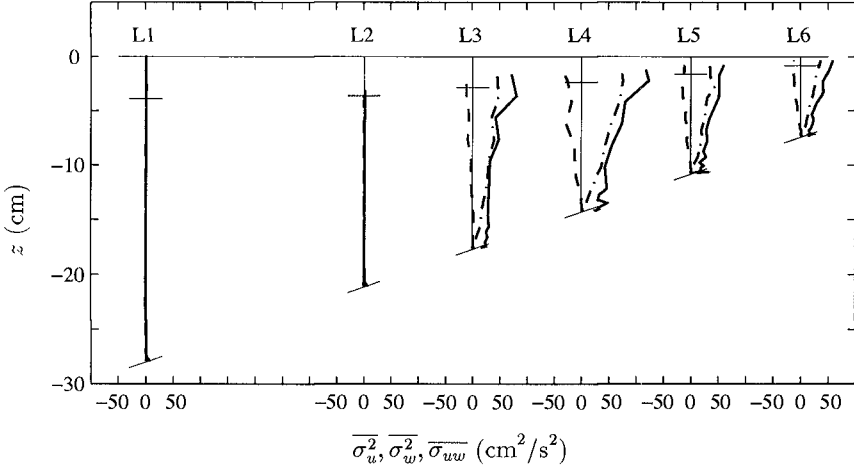


Figure 4: Cross-Shore Comparison of Mean Horizontal and Vertical Velocity Variances and Mean Covariance with σ_u^2 (—); σ_w^2 (---); and σ_{uw} (- -) for L1 to L6.

Assuming that Reynolds averaging is the same as the phase averaging used here, the standard definition of k in terms of the variances is given as

$$k = \frac{1}{2} (\sigma_u^2 + \sigma_w^2 + \sigma_v^2) \quad (12)$$

The transverse velocity variance, σ_v^2 , was not measured for this experiment.

For idealized two-dimensional turbulent flow, $\partial u_3 / \partial x_3 = 0$ so that $\tau_{33} = -\frac{2}{3} \rho k$ and then $\sigma_v^2 = \frac{2}{3} k$. This reduces (12) to

$$k = -\frac{3}{4\rho} (\tau_{11} + \tau_{22}) = \frac{3}{4} (\sigma_u^2 + \sigma_w^2) \quad (13)$$

The use of (10) results in $\frac{1}{2}(\sigma_v^2/k) = \frac{1}{3}$, corresponding to homogeneous isotropic turbulence. For steady turbulent flow, the ratios of the normal stresses to the turbulent kinetic energy have been tabulated by Svendsen (1987). This table indicates that the range is $0.21 \leq \frac{1}{2}(\sigma_v^2/k) < \frac{1}{3}$ so that σ_v^2 may be overestimated slightly here.

Having measured σ_u^2 and σ_w^2 directly, Cox (1995) determined whether the ratio of the vertical to horizontal velocity variance, $C_w = \sigma_w^2 / \sigma_u^2$, is constant over a wave period. The results show that the values lie in the range $0.06 \leq C_w \leq 0.86$ for the variances below trough level whereas the range for the types of flows listed in Svendsen (1987) is $0.16 \leq C_w \leq 1.00$. For L3 to L6, C_w is fairly constant

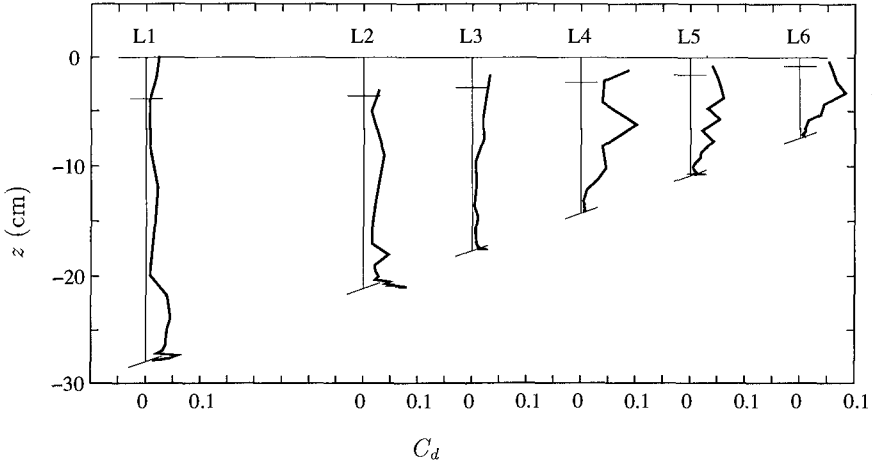


Figure 5: Cross-Shore Variation of C_d for L1 to L6.

over depth with $C_w \simeq 0.7$ until the lower portion of the water column where it decreases linearly toward the rough bottom. Further comparisons of the temporal variations of $C_w \sigma_u^2$ and σ_w^2 similar to Figures 2 and 3 show that it is appropriate to assume that C_w is constant over a wave period in the boundary layer outside the surf zone and below trough level inside the surf zone (Cox, 1995).

A least-squares error method is used to calibrate C_d following (8). Assuming that C_d is independent of time, the least-squares equation is

$$\sqrt{C_d} = \frac{\sum_{j=1}^J |\sigma_{uw}|_j k_j}{\sum_{j=1}^J k_j^2} \quad (14)$$

where j indicates the phase out of $J = 220$ phases. Figure 5 shows the cross-shore variation of C_d for L1 to L6 using (14). The vertical variation of C_d is distinctly different for the three regions: L1 and L2 seaward of breaking, L3 in the transition region, and L4 to L6 in the inner surf zone. For L1 and L2, $C_d \simeq 0.06$ in the bottom boundary layer whereas a similar value $C_d = 0.08$ has been used for steady flows and for oscillatory flows in nonbreaking waves. Above the bottom boundary layer for L1 and L2, the values on the right-hand-side of (14) are near zero so that the estimated values in this region are not useful. For L3 in the transition region, the magnitude of C_d is less than 0.03 over most the water column even though the values for k and σ_{uw} are non-zero. For L4 to L6, a typical value is $C_d \simeq 0.05$ below trough level except in the lower portion where it decreases to a small value.

Eqs. (9) and (2) with the calibrated values of C_d are used to determine C_ℓ in

(3). For this procedure, an error term is computed for a range of C_ℓ by summing the absolute value of the difference of (9) and (2) over the water column at each of the 220 phases. The error term is given as

$$Err(j) = \frac{1}{I} \sum_{i=1}^I \left| (\ell^2 \left| \frac{\partial u}{\partial z} \right|) - (C_d^{1/4} \ell \sqrt{k}) \right|_i, \quad j = 1, 2, \dots, 220 \quad (15)$$

where the index i refers to points in the vertical measuring line. The ranges of C_ℓ were $0.01 \leq C_\ell \leq 0.20$ for L1 and L2 and $0.05 \leq C_\ell \leq 0.45$ for L3 to L6. The value of C_ℓ that gave the least error in (15) was adopted at that phase. Figure 6 shows the temporal variation of the adopted value of C_ℓ at each of the 220 phases for L4. This figure shows the amount of scatter expected for the calibrated C_ℓ and shows that there is a slight variation over the wave period. The bore arrives at $t \simeq 0.6$ s (see also Figure 8 for the relative phases of the free surface elevation in the inner surf zone). The time-average values, $\overline{C_\ell}$, computed for all the measuring lines L1 to L6 are $\overline{C_\ell} = 0.032$ (.021); 0.055 (.041); 0.117 (.065); 0.211 (.105); 0.162 (.081); and 0.172 (.089), respectively, where the standard deviation is given in parentheses (Cox, 1995). This gives an overall value of $\overline{C_\ell} \simeq 0.04$ (0.03) outside the surf zone, and $\overline{C_\ell} \simeq 0.12$ (0.07) in the transition region, and $\overline{C_\ell} \simeq 0.18$ (0.09) for the inner surf zone.

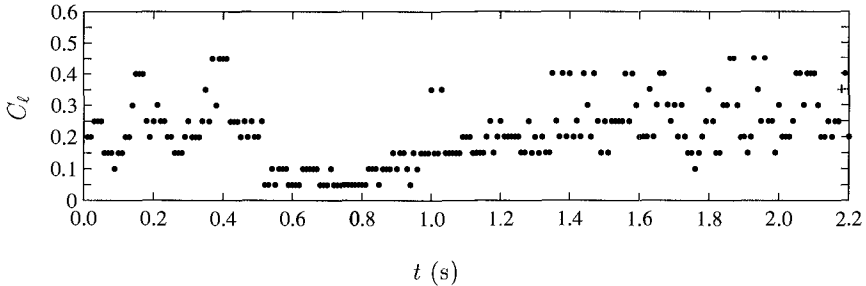


Figure 6: Temporal Variation of Adopted C_ℓ Value at Each of 220 phases for L4 with $\overline{C_\ell} = .211$.

Figure 7 shows the vertical and temporal variations of the eddy viscosity, ν_t , given in (2) computed using the calibrated values of C_d and $\overline{C_\ell}$ for L4. The light vertical lines in the upper figure indicate the extent of the water column at the given phase. The two light horizontal lines in the lower left corner of the top figure indicate the vertical range plotted in detail in the bottom figure. In the bottom figure, z_m is the vertical coordinate from the bottom where $z_m = 0$ on the top of the Plexiglass sheet, i.e. the bottom of the 1 mm sand layer. From both figures, it is clear that ν_t at a given phase increases gradually from the bottom until about the middle of the water column where it is more or less constant

over depth. Also, it is reasonable to assume that ν_t is time-invariant except near trough level with the passing of the bore.

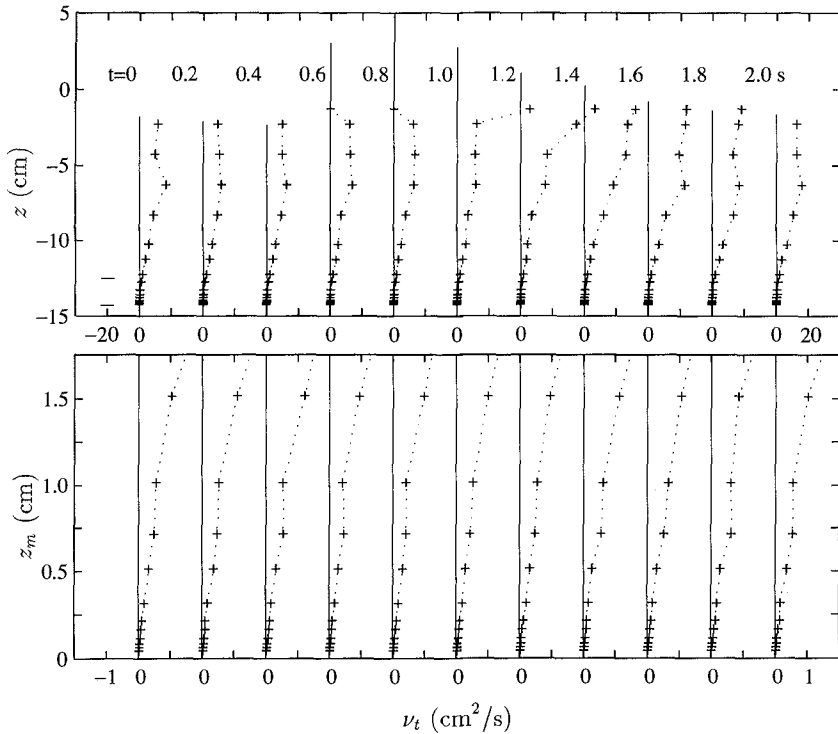


Figure 7: Vertical Variations of Eddy Viscosity, ν_t , at Eleven Phases for L4 with $H^2/T = 30.9 \text{ cm}^2/\text{s}$.

Figure 8 shows the temporal variation of the dissipation term $C_d^{3/4}(k^{3/2}/\ell)$ and the production term $\tau(\partial u/\partial z)$ using the calibrated C_d and \overline{C}_ℓ values for L5. Smoothing was used for the final plot since the contour lines of the unsmoothed values are difficult to discern in black and white (Cox, 1995). Also, only the measuring points above the bottom boundary layer are plotted. This figure shows that the approximate local equilibrium of turbulence is a reasonable assumption for spilling waves in the inner surf zone. It is noted that the numerical derivatives for additional terms in the dimensional equivalent of (6) were computed and that the noise level was on the same order as the quantities of interest.

CONCLUSIONS

Turbulence measurements of spilling waves were presented and used to show that

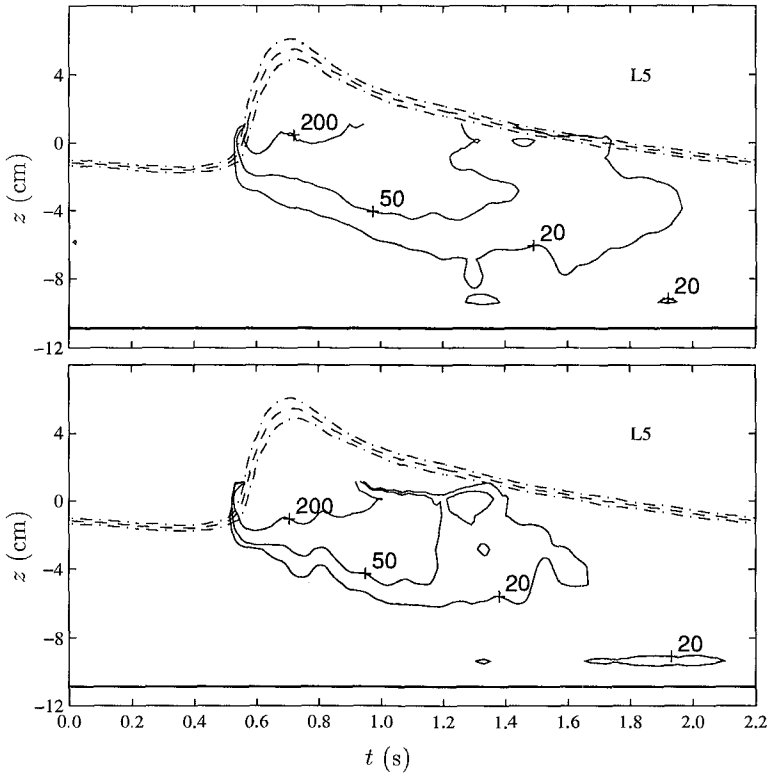


Figure 8: Contour Plot of Temporal Variation of Dissipation Term, $C_d^{3/4}(k^{3/2}/\ell)$, (Top) and Production Term, $\tau(\partial u/\partial z)$, (Bottom) using Calibrated C_d and \overline{C}_ℓ with η_a (—) and $\eta_a \pm \sigma_\eta$ (---) for L5.

the local equilibrium of turbulence is a reasonable approximation for spilling waves in the inner surf zone. Further, the empirical coefficient for the mixing length was shown to be roughly constant over the wave period but varied in the cross-shore direction. The typical values were of $\overline{C}_\ell \simeq 0.04$ (0.03) outside the surf zone, and $\overline{C}_\ell \simeq 0.12$ (0.07) in the transition region, and $\overline{C}_\ell \simeq 0.18$ (0.09) for the inner surf zone. The coefficient related to the dissipation of k was found to be $C_d \simeq 0.06$ in the bottom boundary layer outside the surf zone. In the transition region, the magnitude of C_d was less than 0.03 over most of the water column. In the inner surf zone a typical value was $C_d \simeq 0.05$ over most of the water column except in the lower portion where it decreased to a small value. The eddy viscosity was also shown to increase approximately linearly from the bottom to the middle of the water column where the value became more or less

constant over depth. The eddy viscosity was fairly constant over the wave period except near trough level with passing of the bore.

ACKNOWLEDGMENTS

This work was sponsored by the U.S. Army Research Office, University Research Initiative under contract No. DAAL03-92-G-0116 and by the National Science Foundation under grant No. CTS-9407827. Dr. Okayasu was supported by the Foundation for International Exchanges, Yokohama National University, during his stay at the University of Delaware.

REFERENCES

- ASCE Task Committee on Turbulence Models in Hydraulic Computations (1988). "Turbulence modeling of surface water flow and transport: Part I to V." *J. Hydraulic Engrg.*, ASCE, 114(9), 970-1073.
- Cox, D. T. (1995). "Experimental and numerical modeling of surf zone hydrodynamics." Ph.D. Dissertation, University of Delaware, Newark.
- Cox, D. T., Kobayashi, N. and Okayasu, A. (1995). "Bottom shear stress in the surf zone." in preparation for *J. Geophys. Res.*
- Deigaard, R., Fredsøe, J. and Hedegaard, I. B. (1986). "Suspended sediment in the surf zone." *J. Wtrway. Port Coast. and Oc. Engrg.*, ASCE, 112(1), 115-127.
- Flick, R. E. and George, R. A. (1990). "Turbulence scales in the surf and swash." *Proc. 22nd Coast. Engrg. Conf.*, ASCE, 557-569.
- Fredsøe, J. and Deigaard, R. (1992). *Mechanics of Coastal Sediment Transport*, Advanced Series on Ocean Engineering, Volume 3, World Scientific, New Jersey.
- George, R. A., Flick, R. E. and Guza, R. T. (1994). "Observations of turbulence in the surf zone." *J. Geophys. Res.*, 99(C1), 801-810.
- Launder, B. E. and Spalding, D. B. (1972). *Mathematical Models of Turbulence*. Academic Press, New York, NY.
- Nadaoka, K. and Kondoh, T. (1982). "Laboratory measurements of velocity field structure in the surf zone by LDV." *Coast. Engrg. in Japan*, 25, 125-145.
- Nairn, R.B, Roelvink, J.A. and Southgate, H.N. (1990). "Transition zone width and implications for modelling surfzone hydrodynamics." *Proc. 22nd Coast. Engrg. Conf.*, ASCE, 68-81.
- Okayasu, A. and Cox, D. T. (1995). "Laboratory study on turbulent velocity field in the surf zone over a rough bed." in preparation for *Coast. Engrg. in Japan*.
- Kobayashi, N. and Wurjanto, A. (1992). "Irregular wave setup and run-up on beaches." *J. Wtrway. Port Coast. and Oc. Engrg.*, ASCE, 118(4), 368-386.
- Rodi, W. (1980). *Turbulence Models and Their Application in Hydraulics*. Int'l. Assoc. for Hydraul. Res., Delft, The Netherlands.
- Stive, M. J. F. (1980). "Velocity and pressure field of spilling breakers." *Proc. 17th Coast. Engrg. Conf.*, ASCE, 547-566.
- Svendsen, I. A. (1987). "Analysis of surf zone turbulence." *J. Geophys. Res.*, 92(C5), 5115-5124.